the geneticssociety

www.nature.com/hdy

ARTICLE

Check for updates

The genetic basis of a colorful signal: the polymorphic dewlap of the slender anole (*Anolis apletophallus*)

Renata M. Pirani[1,2,8,9]✉, Carlos F. Arias[2,3,9], John David Curlis[2,4], Daniel J. Nicholson[2,5], Jessica Stapley[6], W. Owen McMillan[2], Christian L. Cox[2,7] and Michael L. Logan[1,2]

© The Author(s), under exclusive licence to The Genetics Society 2025

Organisms often use colorful morphological traits to communicate with members of their own or other species. While "colorful signaling" systems exemplify well-known examples of the evolution of phenotypic diversity, the genetic basis of most of these traits remains unknown. Male lizards of the genus *Anolis* possess a colorful throat fan, or "dewlap", that is flashed during social displays. These displays have been extensively studied in the context of their role in the adaptive radiation of the genus. In contrast, the genetic basis of the *Anolis* dewlap has received relatively little attention. Here, we studied the dewlap of the slender anole (*Anolis apletophallus*) which exhibits a dewlap polymorphism: males have either an entirely orange dewlap ("solid" morph) or a white dewlap with a basal orange spot ("bicolor" morph). To understand the inheritance of this polymorphism, we conducted 99 crosses between individuals from populations that were fixed for one morph (single/fixed/monomorphic) or contained both morphs (mixed/polymorphic). Next, we investigated the genetic architecture of this trait using a pooled population sequencing (Pool-seq) experiment. Our findings indicate that the slender anole dewlap polymorphism is best explained as an autosomal, single-locus, Mendelian trait with the solid morph allele dominant to the bicolor morph allele. Our outlier analysis of the Pool-seq data identified a region strongly associated with this trait and within this region we identified a promising candidate locus—the transcription factor single-minded 1 (*SIM1*)—that may underly the dewlap polymorphism.

Heredity (2025) 134:343–351; https://doi.org/10.1038/s41437-025-00763-z

INTRODUCTION

Colorful signaling traits have evolved in many taxa and are some of the most visually stunning forms of biological diversity. Understanding the mechanisms that have given rise to the immense variation in signaling traits found in nature has become a central theme in behavioral and evolutionary ecology. Previous research has suggested that variation in light environments can drive signal color divergence across space (e.g., darker colors in brighter environments; Leal and Fleishman 2002, 2004; Ng et al. 2013a) and facilitate speciation (McLean and Stuart-Fox 2014). While selection in local environments could potentially drive adaptation of colorful signals to maximize conspicuousness, the way a trait responds to selection is ultimately determined by its genetic architecture (Kokko et al. 2017). As such, studies of the genetic bases of such signals are needed to understand and predict the evolution of colorful traits.

Studies of color pattern polymorphisms, in which multiple discrete color patterns, called "morphs", coexist in a population (Gray and McKinnon 2007), have provided great insight into our understanding of the evolution of animal signaling (Sinervo et al. 2001, 2007; Brock et al. 2020; Pryke 2007; Dijkstra et al. 2009; Maan and Cummings 2008; Prates et al. 2021; Muñoz et al. 2013; Ng et al. 2013a, b, Ng and Glor 2011). The discrete nature of polymorphic phenotypes and the often-clear predictions for morph frequencies in local environments means that polymorphic signaling traits provide excellent systems to study the origin and influence of genetic variation in natural populations of non-model organisms (Hoffman et al. 2006; McLean and Stuart-Fox 2014). Additionally, polymorphic variation, especially in sexual signals, may generate strong effects on mate choice that can accelerate speciation (Prates et al. 2021). Understanding the link between selection on phenotypes and underlying genotypes is crucial for predicting evolutionary trajectories, as this may be the first step in understanding the mechanisms that drive the evolution of reproductive isolation (Stapley et al. 2010). In addition, discrete color traits are often controlled by large effect loci, which simplifies the genotype-to-phenotype map (Wooldridge et al. 2022; Harringmeyer et al. 2023; in prep; Mundy et al. 2016). Thus, systems with polymorphic signaling traits provide excellent opportunities to study the origin and influence of genetic variation in natural populations (Hoffman et al. 2006).

A classic example of a highly diverse, often brightly colored signal is the dewlap of *Anolis* lizards. Dewlaps are folds of skin below the chin that are extended and retracted during signaling

[1]Department of Biology and Program in Ecology, Evolution, and Conservation Biology, University of Nevada Reno, Reno, NV, USA. [2]Smithsonian Tropical Research Institute, Panama City, Panama. [3]Data Science Lab, Office of the Chief Information Officer, Smithsonian Institution, Washington, DC, USA. [4]Department of Ecology and Evolutionary Biology, University of Michigan, Ann Arbor, MI, USA. [5]University of Texas Arlington, Arlington, TX, USA. [6]Department of Environmental Systems Science, ETH Zürich, Zürich, Switzerland. [7]Department of Biological Sciences and Institute of Environment, Florida International University, Miami, FL, USA. [8]Present address: Department of Ecology and Evolutionary Biology, University of California Los Angeles, Los Angeles, CA, USA. [9]These authors contributed equally: Renata M. Pirani, Carlos F. Arias. Associate editor: Rowan Barrett.
✉email: renatampirani@gmail.com

Received: 9 July 2024 Revised: 8 April 2025 Accepted: 10 April 2025
Published online: 30 April 2025

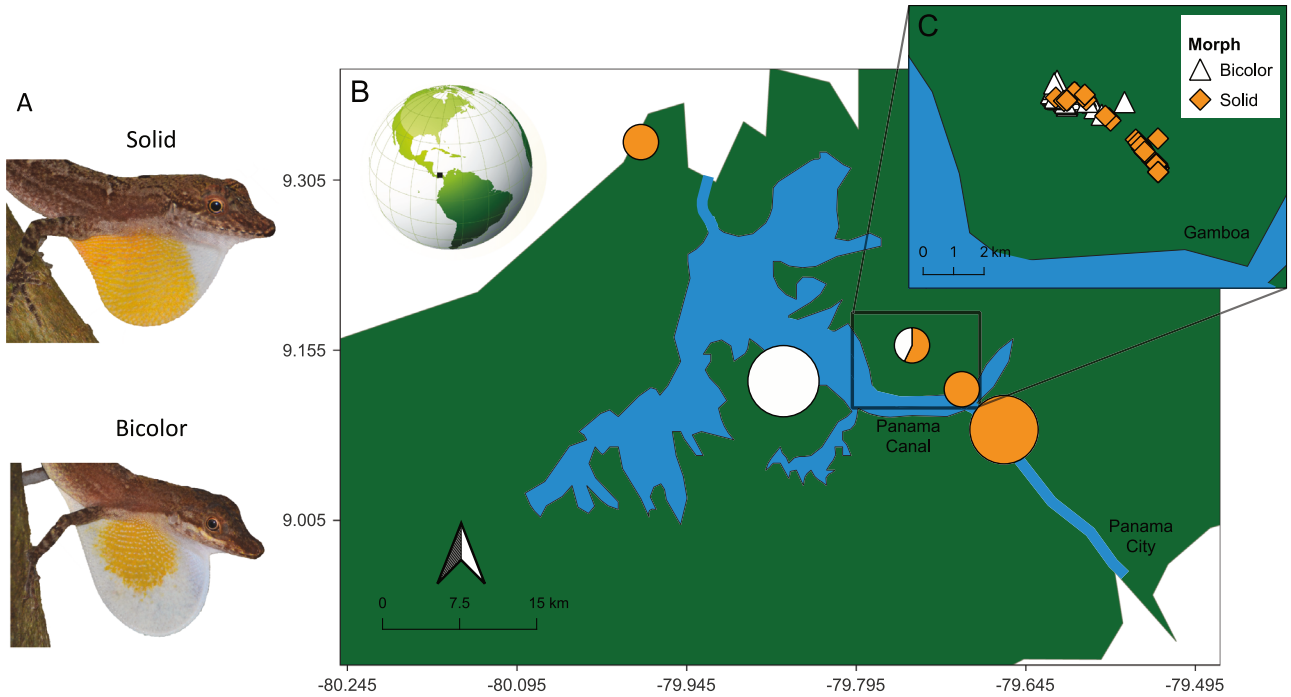

Fig. 1 Distribution of sampling localities for individuals included in our breeding experiment. A Male slender anole dewlaps come in two morphs: solid and bicolor (photographs taken by John David Curlis). **B** Sampling localities in the Canal Zone of central Panama and associated morph frequencies of males in those populations (circle size corresponds to relative sample size from each site). The frequency of solid morph individuals generally declined from the Pacific to the Caribbean versant of Panama. **C** Sampling localities for individuals included in our Pool-seq experiment. All these individuals were collected along a central trail that bisects Soberanía National Park, near the town of Gamboa. For geographic coordinates of all lizard captures, see Tables S1 and S2.

displays, often accompanied by pushups and head-bobbing (Nicholson et al. 2007). Usually, the color pattern of a given dewlap is species-specific (although there is often intraspecific variation; Ng and Glor 2011), and there is a staggering diversity of dewlaps across the genus. Decades of research have implicated this trait in a range of functions, including mate attraction, territory defense, predator deterrence, and species recognition (reviewed in Losos 2009; Ng et al. 2017; Nicholson et al. 2007). Despite the enormous variation in dewlap size and color across anole species, only a small subset have polymorphic dewlaps (e.g., Lambert et al. 2013; Ng and Glor 2011; Ng et al. 2013b; Prates et al. 2015, 2021; Stapley et al. 2011). Notwithstanding their relative rarity, anole species with two or more dewlap morphs offer valuable systems for studying the maintenance of variation, the genetic basis of phenotypic traits, and the selective pressures that drive the evolution of colorful signals. For example, a recent study found that a dewlap polymorphism in the Hispaniolan bark anole (*Anolis distichus*) follows simple Mendelian inheritance (Behere et al. 2024), although the candidate loci or genes underlying this polymorphism are currently unknown.

We studied the slender anole (*Anolis apletophallus*), which is a small arboreal lizard of the forest understory found in lowland tropical forests of central and western Panama (Köhler and Sunyer 2008). Slender anoles are an annual species with adult survival rates of less than 5% (Andrews and Nichols 1990). Males, but not females, of this species are territorial and there is some indirect evidence that they may have a polygynous mating system (Andrews and Rand 1983; Andrews and Stamps 1994). Slender anoles are sexually dimorphic in dewlap expression, with males having large dewlaps and females having no dewlap at all (Rosso et al. 2020). Slender anole dewlaps also show color pattern polymorphism; males either have an entirely orange dewlap (which we call the "solid" morph) or a dewlap that is mostly white but with an orange basal spot near the chin (which we call the "bicolor" morph; Fig. 1A). Populations of slender anoles can have both morphs present (mixed/polymorphic) or be fixed for only one morph (single/fixed/monomorphic) and in general, the frequency of the solid morph declines from the Pacific to the Atlantic coasts of Panama in parallel with a rainfall gradient (Stapley et al. 2011). This geographic variation in dewlap morph frequency may be driven by local adaptation to variation in the light environment (Leal and Fleishman 2002).

To understand the inheritance mode and genetic architecture of this polymorphic signal, we first conducted a laboratory breeding experiment, using both within and between-population crosses, as well as backcrosses, to test the hypothesis that the slender anole dewlap polymorphism is a simple, autosomal, single-locus, Mendelian trait. Second, we searched for loci associated with the polymorphism in slender anoles using pooled population sequencing ("Pool-seq"; Futschik and Schlotterer 2010) anchored with a high-quality draft reference genome (Pirani et al. 2024). Our work provides some of the best information to date on the genetic basis of dewlap coloration in anoles and establishes the slender anole dewlap polymorphism as an important model system to study how local adaptation shapes genetic and phenotypic variation.

METHODS

Testing for mode of inheritance

To establish a breeding colony of slender anoles, we collected lizards from 2011–2013 (primarily during the wet season of each year) at several field sites in the canal region of central Panama (Fig. 1B). Lizards were found by scanning vegetation at heights of approximately 0–2 m in the understory of closed canopy forest. Both adults and sub-adults were collected by hand, placed in a resealable plastic bag, and brought to a Smithsonian Tropical Research Institute (STRI) laboratory facility in the town of Gamboa, Panama. We recorded the sampling location and body size (snout-vent-length and mass) for each individual. We also characterized male dewlap morph by gently grasping the hyoid cartilage with forceps and extending and photographing each dewlap against graph paper. We used the

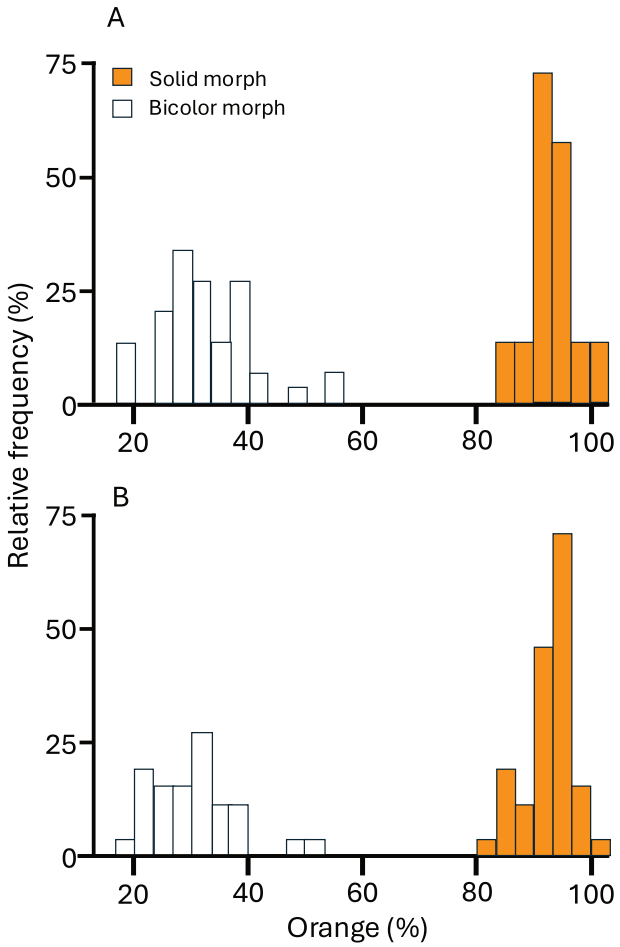

Fig. 2 The percentage of orange in the dewlaps from wild and lab-born males of slender anole. A Wild males from Soberanía National Park, Panama, and **B** lab-born (F1) males, demonstrating that dewlap color pattern in this species is a genetically-controlled, discrete polymorphism. The percentage of orange in the dewlap of slender anoles was discontinuous, with bicolor males possessing less than 60% orange in the dewlap and solid males having greater than 80% orange in the dewlap.

polygon tool in Image J (v1.44; Abramoff et al. 2004) to trace the edges of each dewlap and calculate total dewlap area (in mm^2), as well as the wand tool to measure the area (in mm^2) of orange pigment in each dewlap (Tolerance = 20). We calculated the percentage of orange pigment in each dewlap ($n = 50$ for the bicolor morph and $n = 75$ for the solid morph) and plotted their frequency distributions to confirm that the slender anole dewlap was indeed a bimodally distributed, discrete trait. Based on these distributions (Fig. 2A, B), males were classified as solid if their dewlaps were more than 70% orange.

Lizards were housed individually in cages that were themselves hung inside of an open-sided but shaded outdoor structure on the grounds of the STRI Insectaries in Gamboa, Panama. The temperature, humidity, and light levels inside of lizard cages were similar to the conditions within the forest (wet season: temperature = 22–29 °C, humidity = 80–90%; dry season: temperature = 21–33 °C, humidity = 50–80%). Cages were constructed from pop-up laundry hampers (36 × 36 × 58 cm) that were placed inside handmade mesh bags. Inside each cage were three branches on which lizards could perch and a large artificial leaf to provide a cover object. Cages with females contained a small plastic dish with moist leaf litter (~3 cm deep) for egg deposition. We arranged the cages such that individuals were immediately adjacent to others of the same sex. Lizards could see each other, and dewlap displays were frequently observed. To reduce potential effects of stress from competition, we separated adjacent cages with males (but not females since they appear to be less territorial) with an opaque divider. Every 3 days, all adults were fed 3–6 third and fourth instar crickets, and female cages were checked for eggs (see below for details of our breeding design). All eggs were removed and incubated individually in small plastic cups containing ~1 tablespoon of water and cotton wool, with each egg placed on top of the cotton wool and the cup sealed inside a plastic bag. Eggs were maintained at ambient temperature in an open-air laboratory that experienced similar temperature and humidity conditions to the shaded structure where adult lizards were housed. Eggs were checked daily for hatchlings.

The slender anole has a short generation time for a vertebrate. Eggs hatch in ~44 days and the hatchlings grow quickly, reaching sexual maturity (snout vent length ~ 40 mm) in 4–6 months. Adult survival is less than 5%, so slender anoles are essentially an annual species (Andrews and Nichols 1990). In captivity, after emerging from eggs, hatchlings were weighed and transferred to a ventilated plastic box (180 × 150 × 150 mm). We kept these hatchling boxes in the same shaded structure as adult cages, and each contained three small branches for perching and a plastic leaf as a cover object. Hatchlings were fed size-appropriate crickets (first and second instar). We determined the sex of all juveniles and the dewlap morph of males at about 60 days of age, which is when the dewlap colors become distinguishable. Juveniles remained in hatchling boxes until they reached adulthood (SVL of 40 mm, or ~5 months of age), at which point they were transferred to mesh cages.

To determine the mode of inheritance for dewlap color, we performed a breeding experiment in captivity using a combination of wild-mated females ($n = 13$); lab crosses between wild caught males ($n = 42$) and mostly virgin females (virgin: $n = 25$, non-virgin $n = 6$); and captive born males ($n = 10$) and females ($n = 42$). Female virgin status can be readily confirmed in the lab; mated females produce fertile eggs, whereas virgin females, once mature, produce infertile eggs. Infertile eggs are easily distinguished from fertile eggs, as they are yellow and lack a calcified shell. Six wild caught non-virgin females were also used when they became depleted of wild-male sperm, which could be determined when they stopped producing fertile eggs and only produced infertile eggs.

Our primary hypothesis was that the dewlap morph is controlled by a single large-effect locus. Based on patterns of variation in nature and early observations in the lab, we suspected that it was most likely a Mendelian trait with the solid dewlap allele dominant to the bicolor dewlap allele. Using this model, we denote the solid morph allele as *S* and the bicolor morph allele as *s*, and we made predictions about male offspring morph frequencies from crosses and offspring born in the lab. If our hypothesized model were true, then crosses of $SS \times SS$, $SS \times Ss$, and $SS \times ss$ would result in all sons having the solid dewlap morph, crosses of $ss \times ss$ would result in all sons with a bicolor dewlap morph, and crosses of $Ss \times Ss$ would result in roughly half of the offspring expressing the bicolor dewlap morph and the other half expressing the solid morph.

We first scored the dewlap morph of male offspring born in the lab from wild-mated females originating from monomorphic populations (presumably fixed for either the solid or bicolor morph; $SS \times SS$ or $ss \times ss$). As dewlaps in female slender anoles are usually absent, we assumed that wild-caught females had the homozygous genotype of their source population. The phenotypes of male offspring born from these females would allow us to determine if monomorphic populations breed true to parental types or if there is an environmental component to morph expression. We then performed crosses in the lab between lizards from monomorphic populations ($SS \times ss$ and $ss \times SS$) to create F1 offspring that were presumably heterozygotes at the locus that controls dewlap polymorphism. Scoring dewlap morph in these F1s allowed us to determine if one allele was dominant to the other, if the directionality of these crosses affected phenotypic ratios, if there were maternal or paternal effects, and if sex-linkage was present. Additional crosses between wild-caught individuals of both monomorphic and polymorphic populations were used to further test these patterns. Finally, we performed backcrosses (F1 heterozygotes crossed with the presumed homozygous recessive or dominant parental phenotypes, $F1 \times ss$ or SS) and $F1 \times F1$ ($Ss \times Ss$) crosses to confirm the Mendelian mode of inheritance of dewlap morph. We evaluated the inheritance mode by quantifying observed versus expected dewlap morph ratios of offspring assuming the dewlap polymorphism is controlled by a single autosomal locus with dominance. Differences between observed and expected offspring ratios were evaluated using *chi-square* tests in R (v.4.0.2; R Development Core Team 2023). For each cross type, multiple pairs of lizards were bred and all offspring from each cross type were pooled for analysis. When expected and observed values were zero for one of the offspring phenotypes, no statistical tests were necessary to reject the null hypothesis. We also evaluated observed versus expected ratios after pooling offspring from all crosses to test whether crosses from all genotype combinations produced ratios consistent with

Table 1. Results of slender anole captive breeding experiments.

Type of cross	Dam origin	Sire origin	Sire dewlap morph	Assumed parental genotypes	Male offspring	Obs. solid	Obs. bicolor	Exp. solid	Exp. bicolor	X^2	*P*
Wild mated	Solid	Solid	Solid	*SS x SS*	5	5	0	5	0	NA	NA
Wild mated	Bicolor	Bicolor	Bicolor	*ss* × *ss*	15	0	15	0	15	NA	NA
F0 lab	Mixed	Solid	Solid	? × *SS*	6	6	0	6	0	NA	NA
F0 lab	Solid	Mixed	Solid	*SS* × *S-*	4	4	0	4	0	NA	NA
F0 lab	Solid	Mixed	Bicolor	*SS* × ss	2	2	0	2	0	NA	NA
F0 lab	Solid	Solid	Solid	*SS* × *SS*	2	2	0	2	0	NA	NA
F0 lab	Solid	Bicolor	Bicolor	*SS* × *ss*	10	9	0	9	0	NA	NA
F0 lab	Bicolor	Mixed	Solid	*ss* × *S-*	9	3	6	–	–	NA	NA
F0 lab	Bicolor	Mixed	Bicolor	*ss* × *ss*	0	0	0	0	0	NA	NA
F0 lab	Bicolor	Bicolor	Bicolor	*ss* × *ss*	4	0	4	0	4	NA	NA
F0 lab	Bicolor	Solid	Solid	*ss* × *SS*	18	16	0	16	0	NA	NA
F1 X F1	Lab	Lab	Solid	*Ss* × *Ss*	3	1	2	2.25	0.75	2.77	0.904
Backcross	Lab	Lab (F1)	Solid	*ss* × *Ss*	3	1	2	1.5	1.5	0.33	0.436
Backcross	Lab (F1)	Bicolor	Bicolor	*Ss* × *ss*	7	1	6	3.5	3.5	3.57	0.941
Backcross	Lab (F1)	Solid	Solid	*Ss* × *SS*	6	6	0	6	0	NA	NA
Total	–	–	–	–	94	53	35	57.25	24.75	4.56	**0.96**

We compared observed offspring ratios with expected ratios assuming that the slender anole dewlap polymorphism is an autosomal, single-locus, Mendelian trait with the solid allele (*S*) dominant to the bicolor allele (*s*). When wild-caught solid and bicolor parents were from monomorphic populations (origin = solid or bicolor), we assumed that these individuals were homozygous for the respective morph. For wild-caught males from polymorphic populations (origin = mixed)—males with the solid dewlap phenotype carry at least one dominant allele (*S*), and males with the bicolor dewlap phenotype were homozygote recessive (*ss*). When wild-caught females came from polymorphic populations, we did not assume an a priori genotype. The genotype of lab-born parents (e.g., F1) was assumed based on their parental genotypes. The male offspring that we included in analyses were only those that survived to adulthood. Dams that were either wild-mated and allowed to lay eggs in the lab or wild-caught and crossed in the lab (these dams were virgins or sperm-depleted), and F1 sires and dams that were lab-born and raised and then crossed with each other or back-crossed with homozygous parents.

our a priori hypothesis for mode of inheritance. A detailed breakdown of each cross as well as a summary of sample sizes and statistical results from all cross types are presented in Table 1.

Investigating the genetic architecture of the slender anole dewlap polymorphism

To detect candidate loci underlying the slender anole dewlap polymorphism, we used the Pool-seq approach developed by Futschik and Schlotterer (2010). Pool-seq is an effective method because it has reduced sampling error and provides a high probability of SNP detection across the entire genome (Futschik and Schlotterer 2010; Pfenninger et al. 2015). We compared groups of males from a single mixed-morph population (Fig. 1C), instead of between different fixed-morph populations, to minimize potential confounding effects of among-population genetic structure. From this population, we created two pools, each containing 50 males of either the bicolor or solid dewlap morph (collected from Soberanía National Park in 2019; see Table S2 for the geographic coordinates where all individuals were sampled). We ensured that each individual contributed an approximately equal amount of DNA, which was extracted from tail tips using the Qiagen DNeasy Blood and Tissue Kit following the manufacturer's protocol. Concentration and purity of the extracted DNA was assessed using a Qubit fluorometer (Thermo Fisher Scientific). Two Pool-seq libraries were prepared using the KAPA HyperPlus Kit from 3 µg of total gDNA (60 ng × 50 ind) according to the manufacturer's protocol (Kapa Biosystems). Enzymatic fragmentation was performed for 8 min at 37 °C to obtain an average insert size of 400–500 bp. Single-Indexed Adapters were obtained from KAPA and ligated to fragmented DNA at an adapter: insert ratio of 10:1 (KAPA Single-Indexed Adapter Kit B, Kapa Biosystems). Libraries were amplified for a total of 8 cycles. After amplification, a double-sided size selection (0.5X/0.7X) was performed with Agencourt® AMPure® XP beads (Beckman Coulter). Finally, library size distribution was assessed with a 2100 Bioanalyzer instrument using a High Sensitivity DNA Kit (Agilent Technologies). Each pool was sequenced on a separate Illumina HiSeqX PE150 sequencing lane to achieve close to ~5X coverage per individual in each pool at Genome Quebec (McGill University and Génome Québec Innovation Centre). We ensured high quality of raw reads using the FastQC tool (v.0.11.6; Andrews 2010), using a Phred quality (*Q*) score for all bases of 25 and a mean sequence quality score of 36. All four bases had an even distribution, and the percent of sequence remaining if duplicated was approximately 80% for all libraries.

To filter and align pools to the slender anole reference genome (Pirani et al. 2024), we used the PoolParty pipeline (Micheletti and Narum 2018). Paired-end reads were trimmed to a minimum base quality of 20, and the alignment module *PPalign* was used to align the paired-end reads to the slender anole genome. We also used the *PPalign* module to achieve a minimum sequence length after trimming of 25 base pairs. SNPs were called using a quality score of 15 bp, a minimum depth of 10×, a minor allele frequency (MAF) of 0.05, and an alignment window surrounding each identified indel of 15 bp. We used *PPstats* to assess mapped-read coverage statistics. All bioinformatic analyses were performed on the Smithsonian Institution High Performance Computing Cluster (2023).

To estimate genetic differentiation (pairwise F_{ST} values) and significance of allele frequency differences (Fisher's Exact Test; F_{ET}) for individual reads between the pools representing different dewlap morphs we used the *PPanalyze* module of the PoolParty pipeline (Micheletti and Narum 2018). We calculated allele frequency differences between morphs using a minimum coverage of 4 SNPs and a maximum of 300 SNPs for a minor allele frequency (MAF) of 0.05. This step produced a *sync* output where SNPs that failed comparison specific minimum MAF thresholds were removed. We measured pairwise F_{ST} and sliding-window F_{ST} values using two window sizes: 1000 base pairs (bp) with a 500 bp step and 1 bp with a 1 bp step. We examined differentiation between morphs across the genome, including at a set of recently identified candidate genes related to color and color-pattern in anoles (Table S3, de Mello et al. 2021). We visualized our population genetics results using Manhattan plots in R studio (v.4.0.2). To visualize the distribution of major allele frequencies across all individual pools, we extracted all biallelic SNPs of the candidate

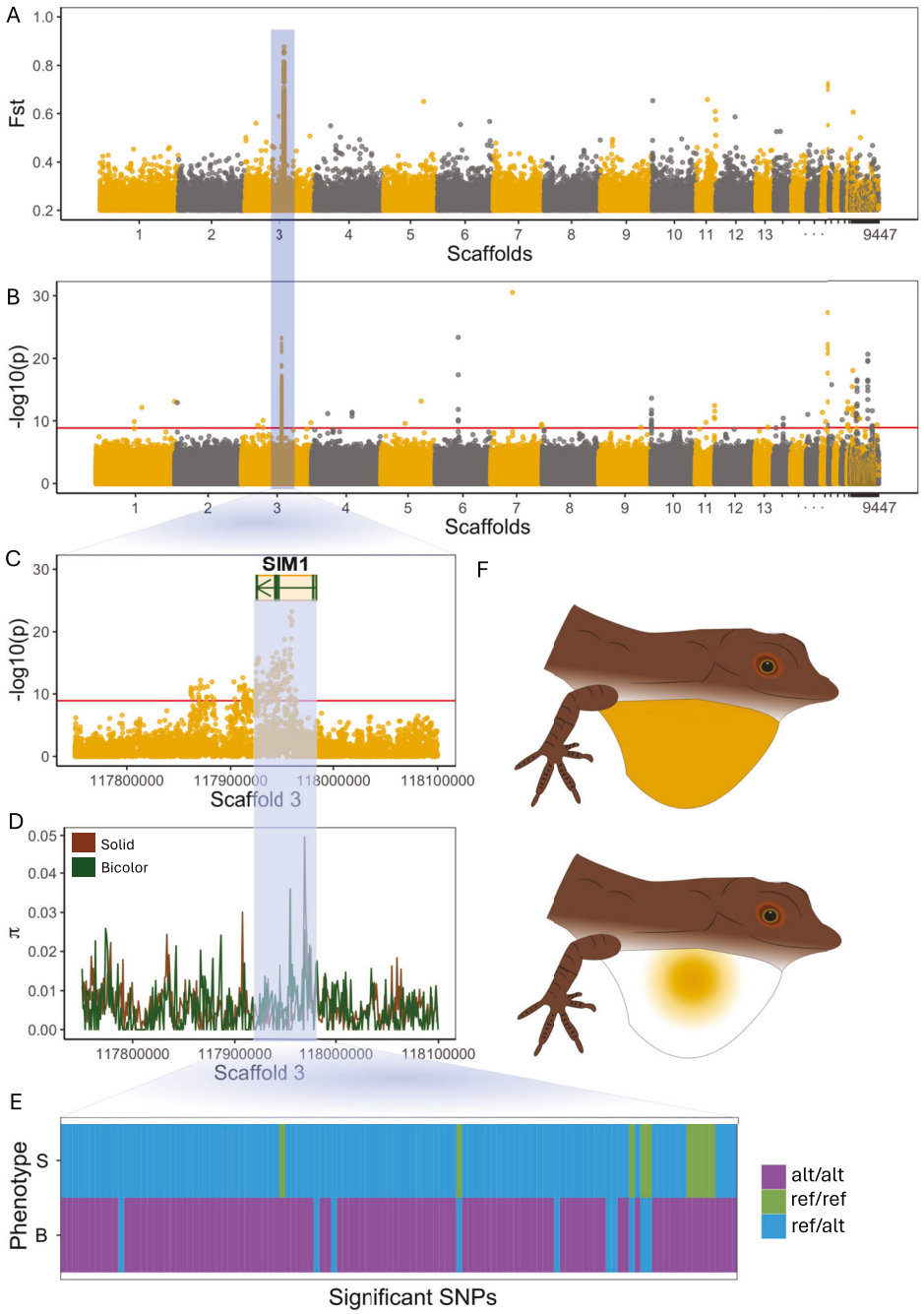

Fig. 3 Pooled sequencing revealed a strong candidate locus (single-minded 1, *SIM1*) that may underly the slender anole dewlap polymorphism. A Manhattan plot illustrating genomic differentiation between the dewlap morphs using pairwise F_{ST} values, and **B** Fisher exact tests. The red lines in **B** and **C** represent the Bonferroni correction (p value = 8.9), with points above the line indicating significantly differentiated SNPs across the slender anole genome. **C** One locus on scaffold 3, the transcription factor *SIM1*, contained a peak of many highly differentiated SNPs between morphs. The vertical green bars in the inset represent exons and the arrow represents the direction of genome annotation. **D** Nucleotide diversity (π) of *SIM1* for the bicolor (green) and solid (brown) dewlap morphs. Note that nucleotide diversity was often higher in the dominant solid morph. **E** SNP panel showing segregating alleles in all significant SNPs (n = 175) in the candidate region of *SIM1* for each morph plotted as a heatmap. We denote ref/ref in green representing that solid morph individuals were fixed for one allele and alt/alt in purple indicates that bicolor individuals were fixed for an alternative allele. Ref/alt in blue represents more than two alleles segregating at that position for either the solid or bicolor population. **F** Male slender anole dewlaps come in two morphs: solid and bicolor.

region (n = 175) and plotted these as heatmap (Fig. 3E). Finally, we re-annotated our slender anole genome using the homology-based gene prediction pipeline GeMoMa (Keilwagen et al. 2016). GeMoMa predicts potential protein-coding genes in a genome or target region by leveraging protein-coding gene models and intron position conservation from reference genomes. We ran the GeMoMa pipeline using annotations from the slender anole (*A. apletophallus*; gene models from Pirani et al. 2024), brown anole (*Anolis sagrei*, rAnoSag1, Geneva et al. 2022), green anole (*Anolis carolinensis*, AnoCar2.0, Alföldi et al. 2011), and common wall lizard (*Podarcis muralis*, PodMur_1.0). All annotations were downloaded from the NCBI genome databases. These species were selected to encompass a range of evolutionary distances, representing both closely and more distantly related high-quality lizard genomes. Additionally, we manually annotated genes and regions of interest (e.g., *SIM1*) by downloading exon

sequences from the green and brown anoles and mapping them to the reference genome using the Geneious mapper (set to high sensitivity and with other parameters set to default; Geneious Prime (2025)).

Molecular signatures of selection

To assess the nucleotide and genetic diversity within each morph, we estimated Tajima's D and π using the variance-sliding script in PoPoolation (v.1.2.2; Kofler et al. 2011) across the candidate genomic regions recovered from the Pool-seq pipeline (see "Results"). We used a sample coverage of 50 for base calls with a minimum *Q*-value of 20 SNPs for these analyses due to the sensitivity of pooled data to variation in coverage and sequencing error (Kofler et al. 2011). For the 1-kb divergence windows of each population pair, we considered the same parameters as described above for pairwise differentiation.

RESULTS

Testing for the mode of inheritance

The percentage of orange pigment in slender anole dewlaps was not related to body size and had a strongly bimodal distribution, confirming the existence of two discrete dewlap morphs in slender anoles as previously reported (Stapley et al. 2011). Summed over all crosses, our breeding experiment yielded 94 male offspring that survived long enough to score their dewlaps (Table 1).

No offspring from any cross had an intermediate dewlap morph, and dewlap morph did not change during ontogeny, suggesting a fixed trait with a simple mode of inheritance and little or no ontogenetic change in this trait. The directionality of the cross did not affect offspring ratios, suggesting that the dewlap locus is autosomal (see Table 1 for a summary of offspring ratios and statistical tests; see Table S1 for details of each individual cross). Offspring born in the lab from females that had mated in the wild within monomorphic populations (expected genotypes $SS \times SS$ or $ss \times ss$, respectively) always produced offspring consistent with the population dewlap morph, indicating that dewlap morph is not environmentally determined, at least within the conditions of our experiment. When presumed homozygotes (from monomorphic populations) for the alternative dewlap morph allele were crossed ($SS \times ss$, or $ss \times SS$), all male offspring had the solid morph phenotype irrespective of whether the paternal or maternal genotype was either *SS* (solid) or *ss* (bicolor). This inheritance pattern, which was further supported by offspring ratios from mating of sires from polymorphic populations with dams from monomorphic populations (and vice versa), was consistent with the solid morph allele being dominant over the bicolor morph allele. When presumed F1 heterozygote offspring (dams and sires produced from crosses between monomorphic solid and bicolor populations) were crossed ($Ss \times Ss$) or backcrossed ($Ss \times ss$, $Ss \times SS$), observed offspring phenotypes did not differ from expected based on a hypothesis of a single-locus, Mendelian-inherited trait with dominance. Finally, after pooling offspring from all cross types, we found that total observed phenotypic frequencies did not significantly differ from expected given our a priori hypothesis for mode of inheritance (Table 1).

Dewlap morph candidate loci

We successfully mapped nearly all pooled sequences to the slender anole reference genome. We had approximately 565 million reads for the bicolor morph and 726 million reads for the solid morph (Table 2). Within the bicolor morph, ~ 530 million bp, corresponding to 94.62% of the genome, were aligned and properly paired for this pool, compared to ~684 million bp (95.01%) for the solid morph. The PoolParty *Ppstats* results for the proportion of the genome covered is shown in Fig. S1.

The alignment module from the PoolParty pipeline resulted in a total of 60,429,504 SNPs before filtering. We removed 7,145,492 SNPs because they were below the minimum threshold for total base quality (20) and total coverage depth (10x). An additional 2,653,066 SNPs were removed because the minor allele frequency was <0.05, leaving a total of 50,630,946 SNPs. Of the remaining SNPs, 6,099,298 were indels. With an indel window of 15 bp (see "Methods") we lost 11,818,072 SNPs or 24% of the remaining SNPs. Lastly, 172,029,724 bp of the reference genome was covered by indel regions.

An outlier plot based on F_{ST} (Fig. 3A) and a Manhattan plot with Fisher Exact Tests (Fig. 3B) revealed several regions of the genome with F_{ST} outliers and SNPs significantly associated with dewlap morph. The regions with the greatest number of highly differentiated SNPs were on scaffolds 3, 17 and 1822. The peak on scaffold 3 was the most prominent (Fig. 3C) and contained the highest number of differentiated SNPs ($n = 175$ significant SNPs with $F_{ET} > 8.9$ after Bonferroni correction). On this scaffold, all significant SNPs were clustered within an approximately 102 kb region, corresponding to the location of the *SIM1* gene. The bulk of the strongly associated SNPs were within introns of *SIM1*, but several fell within exons. While other genes are located nearby (Table S4), unlike the pattern with *SIM1*, there were no significantly differentiated SNPs within the introns or exons of these genes. Analysis of the *SIM1* gene region revealed distinct allelic patterns between the solid and bicolor morphs. Specifically, in the bicolor morph, most positions across this region were fixed for a nucleotide that differed from the reference genome (alternative/alt, purple in Fig. 3E). In contrast, in the solid pool, most positions across this region contained both the reference allele and an alternative allele (reference/alt, blue in in Fig. 3E). Pool-seq does not allow for individual genotyping and the presence of multiple alleles in the solid morph suggests that some individuals in this pool are likely heterozygous, consistent with the dominance of the solid allele over the bicolor allele (see above). Across this region there were only six positions that were fixed for the reference allele in the solid morph (ref/ref, green in Fig. 3E) and the alternative allele in the bicolor morph. Five of these SNPs were clustered within intron 2 of SIM1, coinciding with the peak of differentiation (Fig. 3C, E). In addition, all variable positions within the *SIM1* coding sequence were synonymous changes. Manual curation of this region suggested that some intron and exon regions of the *SIM1* gene that are annotated in the green and brown anoles genomes are missing in the slender anole genome. This did not seem to be associated with an assembly error in the *A. apletophallus* reference genome as we detected no anomalies in our paired-end whole-genome sequencing data across this region and pair-end reads across this region mapped well to our reference. In addition, when we mapped our pool-seq data to the green anole (*Anolis carolinensis)* reference genome, we could detect no reads across these exons.

Scaffolds 17 and 1822 also contained potential candidate loci for controlling the dewlap polymorphism in slender anoles. The differentiated regions on scaffolds 17 (7 SNPs with $F_{ET} > 8.9$ after

Table 2. Summary statistics of pool-seq libraries for the slender anole dewlap morphs.

Dewlap morph	Pool size	Total reads (bp)	Secondary reads (bp)	Mapped reads (%)	Properly paired (bp)	Properly paired (%)	Mate mapped (bp)
Bicolor	50	565,871,403	2,683,685	100	530,918,902	94.62	560,130,392
Solid	50	726,271,514	6,150,693	100	684,159,458	95.01	718,979,815

Bonferroni correction) and 1822 (13 SNPs with $F_{ET} > 8.9$ after Bonferroni correction) corresponded to the genes *CLDN16* (claudin-16, which is a tight-junction protein) and *ZFP2* (ZFP2 zinc finger protein), respectively (Fig. S2). The significant SNPs recovered in all these regions were synonymous mutations within exons. The full list of recovered genes or parts of these genes is in Table S5. We also did not find substantial differentiation at any a priori candidate locus (Table S3) based on its known role in color and color-pattern development when comparing the slender anole genome with the genomes of the green and brown anoles.

Molecular signature of selection

In general, we did not find any obvious molecular signatures of selection in the three genomic intervals that contained outlier loci. Nucleotide diversity (π) within dewlap morphs varied among the three outlier regions but was similar when comparing each candidate region between solid and bicolor morphs (scaffold 3; bicolor: $\pi = 0.006 \pm 0.006$, solid: $\pi = 0.005 \pm 0.006$; scaffold 17: bicolor: $\pi = 0.016 \pm 0.014$, solid: 0.015 ± 0.011; scaffold 1822: bicolor: $\pi = 0.028 \pm 0.006$, solid: 0.025 ± 0.004; Fig. 3D). Genetic diversity (Tajima's *D*) values of the candidate regions (scaffold 3; bicolor: $D = -0.018 \pm 0.152$, solid: $D = -0.039 \pm 0.198$; scaffold 17: bicolor: $D = -0.101 \pm 0.272$, solid: $D = -0.104 \pm 0.273$; scaffold 1822: bicolor: $D = -0.022 \pm 0.054$, solid: $D = -0.113 \pm 0.111$) were similar to genome-wide values (bicolor: min = −3.454, mean = −0.034, max = 2.419; solid: min = −3.439, mean = −0.067, max = 2.148) in both morphs (Fig. S3).

DISCUSSION

Our findings indicate that color pattern polymorphism in the dewlap of the slender anole is a genetically determined phenotype that is inherited as an autosomal, single-locus, Mendelian trait with the solid allele (*S*) dominant over the bicolor allele (*s*). We identified a genomic interval strongly associated with dewlap phenotype. Within this region, the most promising candidate locus for controlling dewlap pattern variation is the transcription factor *SIM1*. To date, little is known about the genetic basis of the *Anolis* dewlap, and our results provide a strong target for future in-depth studies on the proximate mechanisms that drive color variation in this charismatic trait. Furthermore, the simple genetic basis of the slender anole dewlap polymorphism renders this species a potential model system for examining the ecological agents of selection that drive the evolution of colorful signals specifically, and for linking phenotypic and genetic evolution more generally.

In our multi-generational breeding experiment, we did not observe any males with intermediate phenotypes. We also did not observe ontogenetic changes in morph patterns or an effect of the environment. Instead, we found strong evidence in support of the hypothesis that dewlap morph is a discrete and genetically determined trait in this species. All the slender anole offspring born in captivity from crosses between parents that were presumably homozygous for one dewlap morph had the same dewlap morph as their parents. These results were further reinforced by our image analysis, which demonstrated a bimodal distribution in the percentage of orange in dewlaps of wild caught and lab born males. Individuals had either greater than 70% or less than 50% orange pigment (see Fig. 2A, B). A previous study on the Hispaniolan bark anole (*Anolis distichus*) that used intraspecies crosses to assess the relative contributions of genetic and environmental effects on dewlap color found that it was most likely autosomal with dominant or partially dominant alleles (Ng et al. 2013b). It is possible that, within the orange and white portions of the dewlap, color components such as brightness and hue are plastic and respond to exogenous (e.g., parasitism) or endogenous (e.g., hormone concentration) cues, as found in other studies (Cox et al. 2015, 2017; Fitch and Hillis 1984; Nicholson et al. 2007; Vanhooydonck et al. 2009). Regardless, in the slender anole system, whether or not an individual is a solid or bicolor morph appears to be determined entirely by genetics. We also found no evidence of sex-linkage in the inheritance patterns of the slender anole dewlap polymorphism, as offspring ratios followed expectations regardless of the combination of sex and parental genotype. Lastly, we note that several other polymorphic color traits in anoles have simple genetic control. For example, a female-limited polymorphism in dorsal patterning in the brown anole (*Anolis sagrei*) is also an autosomal, single-locus trait (Feiner et al. 2022). In addition, some populations of the Hispaniolan bark anole have a dewlap polymorphism which is similar to that of the slender anole—males of these populations are either solid or bicolor morphs. A recent breeding study demonstrated that this polymorphism is also inherited in a simple Mendelian pattern, with the solid allele dominant to the bicolor allele (Behere et al. 2024). Taken together, these findings suggest that large effect loci with dominance dynamics may frequently underlie color polymorphisms in anoles. However, to our knowledge, our study is the first to reveal candidate gene regions that might be responsible for color variation in dewlaps, specifically.

Male offspring dewlap morph ratios from lab crosses were consistent with the solid allele being dominant to the bicolor allele. First, when presumably homozygous individuals (from monomorphic populations) were crossed with individuals from the alternative monomorphic population, all male offspring were solid morphs. Second, when the individuals from these inter-population crosses (F1s presumed to be heterozygotes, *Ss*) were crossed with each other or backcrossed to a presumed homozygous recessive parent (*ss*), bicolor offspring were produced in proportions that were not significantly different from expected based on dominance of the solid morph allele. Although our results support our hypothesis of Mendelian inheritance with dominance, sample sizes for some crosses were small and thus additional crosses with larger sample sizes might reveal more subtle variation that could indicate the action of additional small effect loci.

Our Pool-seq experiment revealed several candidate regions that might contain loci controlling the slender anole dewlap polymorphism (Figs. 3 and S2). Three loci were highly differentiated between morphs: Claudin-16 (*CLDN16*), ZFP2 Zinc Finger (*ZFP2*), and single-minded 1 (*SIM1*). Of these, *SIM1*, which is a homolog of single-minded 1 in *Drosophila melanogaster*, contained by far the largest number of highly differentiated SNPs (Fig. 3). Because of this pattern, we hypothesize that this locus is like responsible for the observed variation in dewlap pattern in *A. apletophallus* (Fig. 3). The interval spans a 109 kb region, shows evidence for a high degree of linkage disequilibrium among sites, and is focused within intron 2 of *SIM1* (Fig. 3C). The bicolor morph pool that we examined was fixed for a large haplotype that differed from the reference genome at 175 positions (Fig. 3C). This pattern is consistent with the conclusion of our breeding experiment that these individuals are homozygous for the "s" allele.

The function of *SIM1* is not well understood. In the fruit fly, *Drosophila melanogaster*, *SIM1* appears to play a role in the development of the neural system midline cells (Nambu et al. 1991). Nonetheless, it is a DNA-binding transcription factor and is the type of molecule that might play a role in patterning. For example, pattern variation in *Heliconius* butterflies is modulated by several transcription factors, including a homolog of *Optix* (Reed et al. 2011), which before its role in butterfly wing patterning was discovered, was known to be involved in *Drosophila* eye development. Redeployment of transcription factors and other types of signaling molecules to modify developmental functions is common (Dufour et al. 2020). The pattern of association around *SIM1* also suggests the phenotypic change is modulated by *cis*-regulatory variation rather than a change in amino acids in the

protein. *Cis*-regulatory variation is responsible for phenotypic change in a wide range of species including butterflies (Gaunt and Paul 2012), fishes (Gaunt and Paul 2012), birds (Wang et al. 2019), and mice (Wray 2007).

It is possible that the slender anole *SIM1* locus has recently evolved a new function. Our manual curation of this locus suggests that the gene model in the slender anole is significantly different from that of several other anole species. Specifically, the slender anole appears to lack certain exons of this gene compared to brown and green anoles. This deletion falls in the area where we observed the fixed and highly differentiated SNPs, raising the possibility that indel variation directly impacts protein structure or function by altering the coding sequence or disrupting splicing patterns. Detailed gene expression data will be needed to distinguish between these cis-regulatory and protein-coding alternatives. In addition, although *SIM1* remains a top candidate locus, we also identified several other candidate regions and loci (Table S5 and Fig. S2). Similar to *SIM1*, none of these loci have any obvious links to color patterning in any species.

In conclusion, we show that the dewlap polymorphism in the slender anole appears to be inherited in a simple Mendelian fashion, with the solid allele dominant over the bicolor allele. Moreover, we identified a particularly promising gene (*SIM1*) that might underlie the dewlap polymorphism. Additional functional works need to be done to further these findings. CRISPR-Cas9 gene editing, which has recently been used to manipulate coloration in anoles (Ray and Di Felice 2019), seems like a promising approach for identifying the phenotypic effects of the *SIM1* gene. Further research on the functional genomic basis of the slender anole dewlap polymorphism could add new perspectives and generate novel hypotheses for the genetic basis of dewlap color more broadly in *Anolis*, as many species have dewlaps with a similar basal coloration pattern that we see in the bicolor morph of slender anoles (Ingram et al. 2016). Overall, our work represents an important first step is comparative studies on the evolution and function of color-pattern genes among anole species. Ultimately, the simple genetic basis of the slender anole dewlap polymorphism, along with the promising candidate gene that we have identified, indicate that this system is ideal for testing hypotheses about the evolution and maintenance of colorful signals.

DATA AVAILABILITY

Supplementary Material for the breeding and Pool-seq can be found online at the following GitHub repository: https://github.com/renatapirani/Pool-seq-analyses-Anolis-apletophallus. The Pool-seq raw datasets have been deposited in the GenBank database under the accession number PRJNA998426. A more refined annotation has been deposited on our Figshare repository: https://smithsonian.figshare.com/projects/The_genetic_basis_of_a_colorful_signal_the_polymorphic_dewlap_of_the_slender_anole_Anolis_apletophallus_/172950.

REFERENCES

Abramoff MD, Magalhaes PJ, Ram SJ (2004) Image processing with ImageJ. Bioph Int 11(7):36–42

Alföldi J, di Palma F, Grabherr M, Williams C, Kong L, Mauceli E et al. (2011) The genome of the green anole lizard and a comparative analysis with birds and mammals. Nature 477:587–591

Andrews RM, Nichols JD (1990) Temporal and spatial variation in survival rates of the tropical lizard *Anolis limifrons*. Oikos 57:215–221

Andrews RM, Rand AS (1983) Limited dispersal of juvenile *Anolis limifrons*. Copeia 429:434

Andrews RM, Stamps JA (1994) Temporal variation in sexual size dimorphism of *Anolis limifrons* in Panama. Copeia 613:622

Andrews S (2010) FastQC: a quality control tool for high throughput sequence data

Behere A, de Mello P, Geneva AJ, Glor RE (2024) The genetic architecture of dewlap pattern in Hispaniola Anoles (*Anolis distichus*). Evolution 78(5):987–994

Brock KM, Baeckens S, Donihue CM, Martín J, Pafilis P, Edwards DL (2020) Trait differences among discrete morphs of a color polymorphic lizard, *Podarcis erhardii*. PeerJ 8:e10284

Cox CL et al. (2015) Female anoles retain responsiveness to testosterone despite the evolution of androgen-mediated sexual dimorphism. Funct Ecol 29(6):758–767

Cox RM, Costello RA, Camber BE, McGlothlin JW (2017) Multivariate genetic architecture of the *Anolis* dewlap reveals both shared and sex-specific features of a sexually dimorphic ornament. J Evol Biol 30(7):1262–1275

de Mello PLH, Hime PM, Glor RE (2021) Transcriptomic analysis of skin color in anole lizards. Genome Biol Evol 13(7):evab110

Dijkstra PD, Hemelrijk C, Seehausen O, Groothuis TG (2009) Color polymorphism and intrasexual competition in assemblages of cichlid fish. Beh Ecol 20(1):138–144

Dufour HD, Koshikawa S, Finet C (2020) Temporal flexibility of gene regulatory network underlies a novel wing pattern in flies. PNAS 117(21):11589–11596

Feiner N et al. (2022) A single locus regulates a female-limited color pattern polymorphism in a reptile. Sci Adv 8: eabm2387

Fitch HS, Hillis DM (1984) The *Anolis* dewlap: interspecific variability and morphological associations with habitat. Copeia 1984:315–323

Futschik A, Schlotterer C (2010) The next generation of molecular markers from massively parallel sequencing of pooled DNA samples. Gen Soc Am 186(1):207–218

Geneva JA, Park S, Bock D, de Mello PLH, Sarigol F, Tollis M et al. (2022) Chromosome-scale genome assembly of the brown anole (*Anolis sagrei*), an emerging model species. Commun Biol 5:1126

Geneious Prime v.2025.0.3 (2025) Computer software. Biomatters. https://www.geneious.com

Gray SM, McKinnon JS (2007) Linking color polymorphism maintenance and speciation. Trends Ecol Evol 22(2):71–79

Gaunt SJ, Paul YL (2012) Changes in cis-regulatory elements during morphological evolution. Biology 1(3):557–574

Harringmeyer OS, Hu CK, Metz HC, Mihelic EL, Rosher C, Sanguinetti-Scheck J, Hoekstra HE (2023) A single genetic locus lengthens deer mouse burrows via motor pattern evolution. bioRxiv (in preparation)

Hoffman EA, Schueler FW, Jones AG, Blouin MS (2006) An analysis of selection on a colour polymorphism in the northern leopard frog. Mol Ecol 15:2627–2641

Ingram T, Harrison A, Mahler DL, Castañeda MD, Glor RE, Herrel A et al. (2016) Comparative tests of the role of dewlap size in Anolis lizard speciation. Proc Biol Sci Dec 283:20162199

Keilwagen J, Wenk M, Erickson JL et al. (2016) Using intron position conservation for homology-based gene prediction. Nucleic Acids Res 44(9):e89

Kofler R et al. (2011) PoPoolation: a toolbox for population genetic analysis of next generation sequencing data from pooled individuals. PLoS ONE 6(1):e15925

Köhler G, Sunyer J (2008) Two new species of anoles formerly referred to as *Anolis limifrons* (Squamata: Polychrotidae). Herpet 64:91–108

Kokko H, Chaturvedi A, Croll D, Fischer MC, Guillaume F, Karrenberg S et al. (2017) Can evolution supply what ecology demands? Trends Ecol Evol 32(3):187–197

Lambert SM, Geneva AJ, Mahler DL, Glor RE (2013) Using genomic data to revisit an early example of reproductive character displacement in Haitian *Anolis* lizards. Mol Ecol 22:3981–3995

Leal M, Fleishman LJ (2002) Evidence for habitat partitioning based on adaptation to environmental light in a pair of sympatric lizard species. Proc R Soc B 269:351–359

Leal M, Fleishman LJ (2004) Differences in visual signal design and detectability between allopatric populations of *Anolis* lizards. Am Nat 163:26–39

Losos JB (2009) Lizards in an evolutionary tree: ecology and adaptive radiation of anoles. Organisms and environments. University of California Press, Los Angeles, CA

Maan ME, Cummings ME (2008) Female preferences for aposematic signal components in a polymorphic poison frog. Evolution 62(9):2334–2345

McLean CA, Stuart-Fox D (2014) Geographic variation in animal colour polymorphisms and its role in speciation. Biol Rev 89(4):860–873

Micheletti SJ, Narum SR (2018) Utility of pooled sequencing for association mapping in nonmodel organisms. Mol Ecol Resour 18:825–837

Mundy NI, Stapley J, Bennison C, Tucker R, Twyman H, Kim KW et al. (2016) Red carotenoid coloration in the zebra finch is controlled by a cytochrome P450 gene cluster. Curr Biol 26:1435–1440

Muñoz MM, Crawford NG, Mcgreevy JrTJ, Messana NJ, Tarvin RD, Revell LJ et al. (2013) Divergence in coloration and ecological speciation in the *Anolis marmoratus* species complex. Mol Ecol 22:2668–2682

Nambu JR, Lewis JO, Wharton KA, Crews ST (1991) The Drosophila single-minded gene encodes a helix-loop-helix protein that acts as a master regulator of CNS midline development. Cell 67(6):1157–1167

Nicholson KE, Harmon LJ, Losos JB (2007) Evolution of *Anolis* lizard dewlap diversity. PLoS ONE 2:e274

Ng J, Geneva AJ, Noll S, Glor RE (2017) Signals and speciation: *Anolis* dewlap color as a reproductive barrier. J Herp 51(3):437–447

Ng J, Glor RE (2011) Genetic differentiation among populations of a Hispaniolan trunk anole that exhibit geographical variation in dewlap colour. Mol Ecol 20:4302–4317

Ng J, Landeen EL, Logsdon RM, Glor RE (2013a) Correlation between *Anolis* lizard dewlap phenotype and environmental variation indicates adaptive divergence of a signal important to sexual selection and species recognition. Evolution 67:573–582

Ng J, Kelly AL, MacGuigan DJ, Glor RE (2013b) The role of heritable and dietary factors in the sexual signal of a Hispaniolan anolis lizard, *Anolis distichus*. J Hered 104(6):862–873

Pfenninger M, Patel S, Arias-Rodriguez L, Feldmeyer B, Riesch R, Plath M (2015) Unique evolutionary trajectories in repeated adaptation to hydrogen sulphide-toxic habitats of a neotropical fish (*Poecilia mexicana*). Mol Ecol 24:5446–5459

Pirani RM, Arias CF, Charles K, Chung AK, Curlis JD, Nicholson DJ et al. (2024) A high-quality genome for the slender anole (*Anolis apletophallus*), an emerging model for field-studies of tropical ecology and evolution. G3 l(1):jkad248

Prates I, D'Angiolella A, Rodrigues MT, Melo-Sampaio PR, de Queiroz K, Bell RC (2021) Evolutionary drivers of sexual signal variation in Amazon Slender Anoles. Evolution 75(6):1361–1376

Prates I, Rodrigues MT, Melo-Sampaio PR, Carnaval AC (2015) Phylogenetic relationships of Amazonian anole lizards (Dactyloa): taxonomic implications, new insights about phenotypic evolution and the timing of diversification. Mol Phylogenet Evol 82:258–268

Pryke SR (2007) Fiery red heads: female dominance among head color morphs in the Gouldian finch. Behav Ecol 18(3):621–627

Ray A, Di Felice R (2019) Molecular simulations have boosted knowledge of CRISPR/Cas9: a review. J Self Assem Mol Electron 7(1):45–72

Reed RD, Papa R, Martin A, Hines HM, Counterman BA, Pardo-Diaz C, Jiggins CD, Chamberlain NL, Kronforst MR, Chen R, Halder G, Nijhout HF, Mcmillan WO (2011) *optix* drives the repeated convergent evolution of butterfly wing pattern mimicry. Science 333:1137–1141

R Development Core Team (2023) R: a language and environment for statistical computing. Vienna, austria: R Foundation for Statistical Computing

Rosso AA, Nicholson DJ, Logan ML, Chung AK, Curlis JD, Degon ZM, Knell R, Garner TWJ, McMillan WO, Cox CL (2020) Sex-biased parasitism and expression of a sexual signal. Biol J Linn Soc 131:785–800

Sinervo B, Bleay C, Adamopoulou C (2001) Social causes of correlational selection and the resolution of a heritable throat color polymorphism in a lizard. Evolution 55(10):2040–2052

Sinervo B, Heulin B, Surget-Groba Y, Clobert J, Miles DB, Corl A, Davis A (2007) Models of density-dependent genic selection and a new rock-paper-scissors social system. Am Nat 170(5):663–680

Smithsonian Institution High Performance Computing Cluster (2023) Smithsonian Institution. https://doi.org/10.25572/SIHPC

Stapley J, Reger J, Feulner PGD, Smadja C, Galindo J, Ekblom R et al. (2010) Adaptation genomics: the next generation. Trends Ecol Evol 25(12):705–712

Stapley J, Wordley C, Slate J (2011) No evidence of genetic differentiation between anoles with different dewlap color patterns. J Hered 102(1):118–124

Vanhooydonck B, Herrel A, Meyers JJ, Irschick DJ (2009) What determines dewlap diversity in *Anolis* lizards? An among-island comparison. J Evol Biol 22:293–305

Wang Q, Jia Y, Wang Y et al. (2019) Evolution of cis- and trans-regulatory divergence in the chicken genome between two contrasting breeds analyzed using three tissue types at one-day-old. BMC Genomics 20(933):1–10

Wooldridge TB, Kautt AF, Lassance JM, McFadden S, Domingues VS, Mallarino R, Hoekstra HE (2022) A novel enhancer of *Agouti* contributes to parallel evolution of cryptically colored beach mice. PNAS 119(27):e220286119

Wray G (2007) The evolutionary significance of cis-regulatory mutations. Nat Rev Genet 8:206–216

ACKNOWLEDGEMENTS

The authors would like to thank Guillermo Garcia-Costoya for help with analyses. We would also like to thank the staff of the Smithsonian Tropical Research Institute for logistical support. This work was supported by the National Science Foundation (award numbers DEB-2024157 to MLL, DEB-2024179 to CLC, and DEB-2024109 to WOM), Smithsonian Institution Biodiversity Genomics and Earl S. Tupper Fellowships (MLL), and grants from the Smithsonian Tropical Research Institution (WOM, MLL, JDC, DJN, and CFA). Marie Skłodowska-Curie International Fellowship to JS (253300). We thank four anonymous reviewers for insightful feedback that helped us improve the manuscript.

AUTHOR CONTRIBUTIONS

RMP, JS, WOM, CLC, and MLL conceived the project. RMP, CFA, JDC, DJN, CLC, and MLL collected tissues and supported the project logistically. JS performed the breeding experiment. RMP and CFA performed statistical and bioinformatics analyses. RMP wrote the first draft of the manuscript, and all authors contributed to manuscript revision.

COMPETING INTERESTS

The authors declare no competing interests.

RESEARCH ETHICS STATEMENT

All animal procedures followed the 1964 Helsinki Declaration and were performed in accordance with ethical approval from the Smithsonian Tropical Research Institute (IACUC protocol numbers 2011-0326-2013-05 and 2020-0601-2023-A2).

ADDITIONAL INFORMATION

Supplementary information The online version contains supplementary material available at https://doi.org/10.1038/s41437-025-00763-z.

Correspondence and requests for materials should be addressed to Renata M. Pirani.

Reprints and permission information is available at http://www.nature.com/reprints

Publisher's note Springer Nature remains neutral with regard to jurisdictional claims in published maps and institutional affiliations.

Springer Nature or its licensor (e.g. a society or other partner) holds exclusive rights to this article under a publishing agreement with the author(s) or other rightsholder(s); author self-archiving of the accepted manuscript version of this article is solely governed by the terms of such publishing agreement and applicable law.